Iraqi Journal of Science, 2025, Vol. 66, No. 11, pp: 5045- 5057
DOI: 10.24996/ijs.2025.66.11.29

ISSN: 0067-2904

Mathematical Modeling to Study the Impact of the Magnetic Field on the Axial Velocity and Flow Function of Non-Newtonian Walter's-B Fluid Through Curved Peristaltic Channels

Zainab A. Jaafar[1*], Hana I. Lafta[2]
[*1] *Department of Physics, College of Education /Tuz Khurmatu, Tikrit University, Tikrit, Iraq*
[2] *Department of Mathematic, Diyala Education Directorate, Diyala, Iraq*

Received: 2/3/2024 Accepted: 13/10/2024 Published: 30/11/2025

Abstract

In this research, we analyzed the effect of the magnetic field on the axial velocity function, as well as the stream function of non-Newtonian Wallers-B fluid in the inner duct and walls of curved peristaltic channels. This model was examined assuming along wave length and a low Reynolds number relative to a small Brinkman number (Br) using the modern and effective technique of the Mathematica program, the exact solutions of the governing partial differential equations were found. After they were converted to ordinary differential equations. We verified the numerical results through the graphs of all the physical parameters and used the regular perturbation method to reach the numerical solutions for both the axial velocity and flow functions, we conducted the discussion based on the graphs obtained in the Mathematica soft ware for the relevant parameters and it turned out that they are parabolas where the velocity increases with the increasing the parameters values for the curved walls and the behaviour here seems some what oscillatory with increasing the curvature parameter .

Key words: Curved peristaltic channels, Constitutive equations, Walter's- B fluid, Long wave length , Brinkmann number (Br) ..

لمائع والتر B اللاينوتوني عبر القنوات التمعجية المنحنية

زينب علي جعفر[1*], هناء لفته ابراهيم[2]
[1*]قسم الفيزياء,كلية التربية طوزخورماتو,جامعة تكريت,تكريت,العراق
[2]قسم الراضيات, مديرية تربية ديالى,ديالى, العراق

الخلاصة

في هذا البحث قمنا بتحليل تأثير المجال الفناطيسي في دالة السرعة المحورية وكذالك دالة الجريان لمائع والتر B اللانيوتوني في المجرى الداخلي وجدران القناة التمعجية المنحنية . ثم فحص هذا النموذج بأفتراض طول الموجه الطويل وعدد رينولدز المنخفض، بالنسبة لعدد برينكمان (Br) الصغير وبأستخدام التقنية الحديثة والفعالة لبرنامج المايثماتكا تم إيجاد الحلول الدقيقة للمعادلات التفاضلية الجزئية الحاكمة بعد ان تم تحويلها الى معادلات تفاضلية اعتيادية. وتحققنا من النتائج من خلال الرسوم البيانية لجميع المعلمات الفيزيائية وقد استخدمت طريقة الاضراب المنتظم في التوصل الى الحلول العددية لكل من دالتي السرعة المحورية ودالة

*Email: zainabali611@tu.edu.iq

الجريان. أجرينا المناقشة بالاعتماد على الرسوم المستحصلة في برنامج المايثماتكا للمعلمات ذات الصلة وتبين انها قطوع مكافئة حيث تزداد السرعة بزيادة قيم المعلمات للجدران المنحنية والسلوك هنا يبدو نوعا ما متذبذبا بازدياد معلمة الانحناء.

1. Introduction

As for the waves that propagate along the walls of the flexible channels, they will contribute to the continuity of flow without the need to rely on external pressure gradients. Such flows, which are called peristaltic flow, can be observed in most areas of the human body, for example, the digestive system, the urinary system, the reproductive system, the female fallopian tube, the kidney tubules, and many others. For this reason, the study of peristaltic transport has been and continues to be a subject of study and research, as it has received the largest share of researcher's attention fluids a like. In fluid mechanics, the fact has emerged that confirms that most physiological fluids we deal with as if they were non-Newtonian fluids, and there are many theological models that have been studied in the recent past, which are models for inelastic fluids, for example bul not limited lathe plastic Bingham and power law model and the viscoelastic fluid which are models arranged like the maxwell model, the oldroyd-B model and the Jahuson- seyalman mudel. In this research article, the effect of various thelogical factors on the function of pristaltic pumping was studied. It can be said that the theological models used in previous studies and research do not have the strength of flow free of distortions, as peristaltic flows consist of a series of enverging and diverging flows spread in channels, So our study here will be somewhat typical of flows in curved channels. Peristaltic transport in curved channels of fluids is a topic of interest to researchers, physiologists and engineers, becouse of its physiological and engineering effects. Peristaltic transport has been defined by mathematicians as a mechanism for transporting fluids resulting from a wave that develops between contraction and relaxation along the length of an expandable tube. Due variety of applications[1-5].

It is important to mention that peristaltic transport within the curved channels is abiological mechanism responsible for various physiological functions of the organs of the human body. This mechanism is represented by the passage of urine from the kidneys to the bladder, the movement of the egg in the fallopian tube, in addition to the transport of lymph in the lymphatic vessels, and the transport of sperm in the ducts of the male reproductive system. In practice, peristaltic pumps are manufactured to transport rheological fluids in various industries, as they separate fluids that cause corrosion and harmful fluids, in addition to transporting sensitive fluids in the treatment of cancerous diseases. The effect of both the axisymmetric magnetic field and the applied magnetic field on peristaltic flows is of utmost importance in treating many of the problems of physiological conductive fluid movement, including, for example, blood, the industrial blood pump machine, and targeting magnetic medical drugs related to the organs of the human body, especially with regard to the treatment of partial paralysis of the stomach and chronic constipation. In addition to contemporary diseases (morbid obesity). Therefore, the impact of heat transfer in peristaltic transport within a curved channel is of great importance in food oxygenation, kidney dialysis, tissue conduchion, and convection in wood from all tissue pores, in addition to thermal radiation between the environment and its surface, and how to treat it [6-11].

There are many methods of peristaltic transport present in the processes of distillation, scattering of chemical impurities, membrane separation processes, and combustion. It is naled that the main relationships accur between flows and driving potentials when mass and heat transfer work at the same time, as the gradient in temperature distribution generates flows of

energy, and despite this is because the mass flow and composition gradients are due to the main cause, which is the gradient in the temperature distribution, which is called the phenomenon, (Ulcer effect). The flow of non-Newanian fluids in curved channels has a clear impartin most scientific, engineering and medical disciplines especially industrial, environmental and biologic applications. Among them we mention the flow of floods, related to the to the movement of sediments. The curved geometric shape. Has wide spread importance given that the channels and pipes used in industries and medicine have many bends. We can say that the air craft wings and the turbine engine view the flow through their curved walls as having technical advantages, especially with the curvature parameter (k) [12], [13]. Other examples include the spread of pollution in straits and complex marine terrain - it may be very appropriate to benefit from flow analysis in curved. Peristaltic channels in most practica studies. However, there is little literature on this perspective.The conservation equations for curved coordinat form complex non-linear differential equations. This has been studied by [14]. As well as by Khan ad presented a peristaltic movement of a dusty fluid a curved configuration with mass transfer [15]. Anibren et al. had provided the study of Jeffery fluid in a curved channel, they have been investigated in effect of relaxation and retardation times on dusty Jeffrey fluid in acurved channel under the influence of a radically changing magnetic field [16]. Other vital studies the effect of the magnetic field on the dynamic velocity filed and the flow function of a Walter's -B non-Newtonian fluid through a curved channel [17-19]. Despite the huge amount of literature in this research, the reliance was on the non-curved channel and neglecting the curved channel, and this was not a good thing with regard to the flow of this fluid, so we focused in our current work on a fast converging numerical a pproach to a ddress this problem in the curved channel, noting that researchers had not addressed it previously, which explain its novelty.
In this study we will adopt the non- Newtonian Walter's-B model, to study the effect of viscoelasticity on laminar peristaltic flows. The purpose of this is to simulate the physiological systems present in the human body in more detail, we will assume that the flow path is curved with a curvature parameter (K). Moreover, we study the effect of the radial magnetic field on the peristaltic flow due to the increasing uses of magnetic therapy for cases pathogenesis. We assumed that the viscosity is variable, taking into account the effects of the radial magnetic field on the flow in the curved channel of non-Newtonian Walter's-B fluid, and then studying the effect of the flow function, temperature distribution and pressure gradient. By describing the Brinkmann number (B_r), the Prandtl number (P_r) and the Eckert number (E_C), we were able to solve the constitutive equations using the regular perturbation method and show that effect graphically by collecting graphic shapes using "MATHEMATICA" software.

2. Mathematical formulation

Take into consideration the two-dimensional peristaltšis movement of an viscous in compressible Walter's-B fluid in a curved channel of a thickness (2a), that convolves into a circle with a radial (R) and (o) as a center. Peristalsis flow was created in the curved channel due to the transverse deflections of waves of wave nature with limited amplitudes (b), which were placed on the e Lastic walls of the channel, see Figure (1). It is obvious that the internal effects are relatively small, knowing that the temperature ($T_\circ$) of the channel walls remains equal. The two wall equations are described as follows.

$$\bar{R} = \bar{H}_1(\bar{x}, \bar{t}) = a + b \sin\left(\frac{2\pi}{\lambda}(\bar{x} - ct)\right), \qquad \text{Outer wall,}$$
$$\bar{R} = \bar{H}_2(\bar{x}, \bar{t}) = -a - b \sin\left(\frac{2\pi}{\lambda}(\bar{x} - ct) + \phi\right), \qquad \text{Inner wall,} \tag{1}$$

where overline $\bar{x}$, $\bar{R}$, a , b , λ are presents the axial distance, the radial, the radius of the stationary curved channel, the wave amplitude and the wavelength is increasing compared with the channel width as ($\frac{a}{\lambda} \ll 1$).

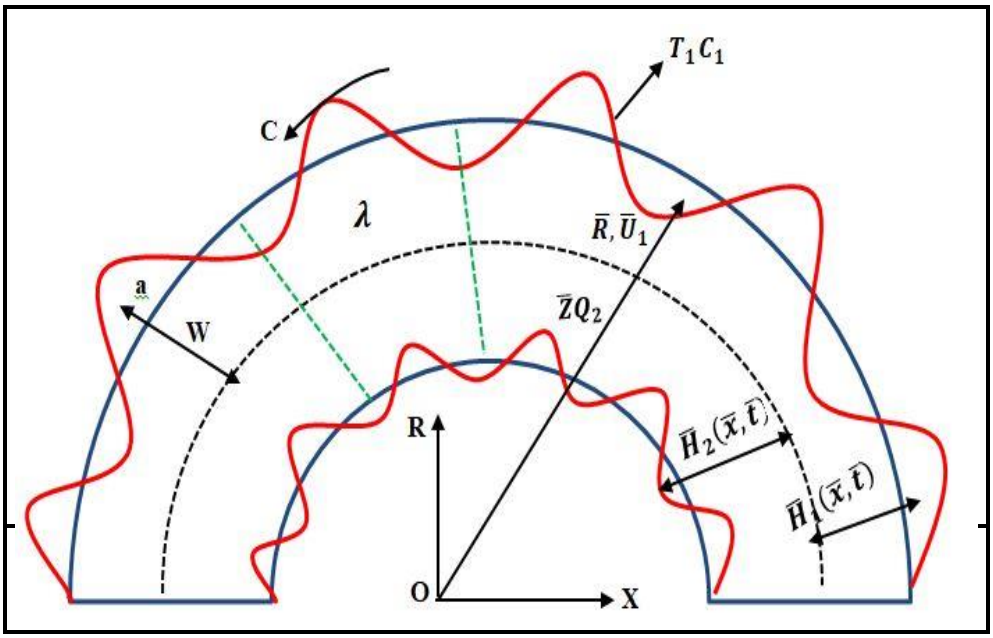

Figure 1: Physical sketch of fluid flow in a curved channal

The propagation wave dominates the fluid flowing towards the left, where each of $U(R\,,X\,,t)\&\,V(R\,,X\,,t)$ represents the components of the velocity in the a zimuthal and radial directions, respectively. In addition to the movement of the peristalsis walls, they are exposed to a magnetic field ($B_\circ$) in the radial direction, assuming that the width of channel is in finitely perpendicular to the plane, so that the fluid can flow uniformly. We can say that the channel is two-dimensional and the fluid is incompressible. In this system, the fluid flow has low Reynolds numbers and the flow is laminar.

3. Constitutive equation:

Basic equations for Walter's-B fluid with unsteady viscosity of temperature can be given as [3] :

$$\tau = 2\eta_\circ w - 2k_\circ w^*. \tag{2}$$

Where

$$w = \nabla\bar{V} + (\nabla\bar{V})^T.$$

$$w^* = \frac{\partial w}{\partial t} + (V.\nabla)w - w.\nabla V - (\nabla V)^T w. \tag{3}$$

$$\frac{R^\circ}{r+R^\circ}\frac{\partial\bar{u}}{\partial\bar{x}} + \frac{\partial\bar{v}}{\partial\bar{r}} + \frac{\bar{v}}{\bar{r}+R^\circ} = 0. \tag{4}$$

$$\rho\left(\frac{\partial\bar{v}}{\partial\bar{t}} + \bar{V}\frac{\partial\bar{v}}{\partial\bar{r}} + \frac{UR^\circ}{\bar{r}+R^\circ}\frac{\partial\bar{v}}{\partial\bar{x}} - \frac{U^{-2}}{\bar{r}+R^\circ}\right) = -\frac{\partial\bar{p}}{\partial\bar{r}} + \frac{1}{\bar{r}+R^\circ}\frac{\partial}{\partial\bar{r}}([\bar{r}+R^\circ]\bar{\tau}_{\bar{r}\bar{r}}) + \left(\frac{R^\circ}{\bar{r}+R^\circ}\right)$$

$$\frac{\partial\bar{\tau}_{\bar{r}\bar{x}}}{\partial\bar{x}} - \frac{1}{\bar{r}+R^\circ}\bar{\tau}_{\bar{x}\bar{x}}. \tag{5}$$

$$\rho\left(\frac{\partial\bar{u}}{\partial\bar{t}}+\bar{V}\frac{\partial\bar{u}}{\partial\bar{r}}+\frac{\bar{u}R^{\circ}}{\bar{r}+R^{\circ}}\frac{\partial\bar{u}}{\partial\bar{x}}-\frac{\bar{u}\bar{v}}{\bar{r}+R^{\circ}}\right)=-\left(\frac{R^{\circ}}{\bar{r}+R^{\circ}}\right)\frac{\partial\bar{p}}{\partial x}+\frac{1}{(\bar{r}+R^{\circ})^{2}}\frac{\partial}{\partial\bar{r}}[(\bar{r}+R^{\circ})^{2}\bar{\tau}_{\bar{r}\bar{x}}]$$
$$+\frac{R^{\circ}}{\bar{r}+R^{\circ}}\frac{\bar{\tau}_{\bar{x}\bar{x}}}{\partial\bar{x}}-\left(\frac{R^{\circ}}{\bar{r}+R^{\circ}}\right)^{2}B_{\circ}^{2}\bar{u}\sigma \quad (6)$$

We will change the reference frame of the coordinate system to the wave frame format and consider the flow in the channel constant by applying the following assumptions:

$$x=X-ct\ ,\ u=U-c\ \ ,\ v=V\ ,\ p=P. \quad (7)$$

To simplify the Equations (4-6), we may introduce the following dimensionless transformations as follows:

$$\bar{x}=\lambda x\ ,\ \bar{r}=ar\ \ ,\ \bar{u}=cu\ ,\ \bar{v}=S_{c}v\ ,\bar{t}=\frac{\lambda t}{c}$$
$$\bar{h}_{1}=a\bar{h}_{1}\ ,\ \bar{h}_{2}=a\bar{h}_{2}\ \ S=\frac{a}{\lambda}\ ,\ R^{\circ}=ak\ ,\ \emptyset=\frac{b}{a}$$
$$\bar{\eta}(T)=\eta_{\circ}\eta(\theta)\ ,\bar{P}=\frac{p\eta_{\circ}c\lambda}{a^{2}}\ ,R_{e}=\frac{pca}{\eta_{\circ}} \quad (8)$$
$$H_{a}=\frac{\sigma a^{2}B_{\circ}^{2}}{\eta_{\circ}}\ \ ,\ \ \bar{\tau}=\frac{\tau\eta_{\circ}c}{a}\ \ ,\ \ P_{r}=\frac{\eta_{\circ}C_{p}}{k_{1}}\ \ ,E_{C}=\frac{C^{2}}{C_{P}T_{\circ}}\ ,B_{r}=P_{r}E_{C}\ ,$$
$$u=-\frac{\partial\psi}{\partial r}\ ,V=S\frac{k}{r+k}\frac{\partial\psi}{\partial x},$$

where k is the curvature parameter, ϕ is the amplitude ratio, by substituting Equations (7 -8) into equations (4 - 6) , we have:

$$k\frac{\partial u}{\partial x}+(r+k)\frac{\partial v}{\partial r}+V=0. \quad (9)$$

$$SR_{e}V\frac{\partial v}{\partial r}S^{2}R_{e}\frac{k(u+1)}{(r+k)}\frac{\partial v}{\partial x}-SR_{e}\frac{(u+1)^{2}}{(r+k)}=-\frac{\partial p}{\partial r}+\frac{S}{(r+k)}\frac{\partial}{\partial r}[(r+k)\tau_{rr}]$$
$$+S^{2}\left(\frac{k}{r+k}\right)\frac{\partial\tau_{rr}}{\partial x}-\frac{S}{(r+k)}\tau_{rr}. \quad (10)$$

$$R_{e}S\left[V\frac{\partial u}{\partial r}+\frac{k(u+1)}{(r+k)}\frac{\partial u}{\partial x}-\frac{V(u+1)}{(r+k)}\right]=-\frac{\partial p}{\partial x}+S\frac{\partial\tau_{rr}}{\partial x}+\frac{1}{k(r+k)}\frac{\partial}{\partial r}$$
$$[(r+k)^{2}\tau_{xr}]-\frac{k^{2}(u+1)}{(r+k)^{2}}H_{a}\ . \quad (11)$$

$$\bar{\tau}_{rr}=4\eta_{\circ}\frac{\partial\bar{v}}{\partial\bar{r}}-2k_{0}\left[2\frac{\partial\bar{v}}{\partial\bar{r}\,\partial\bar{t}}+2\left(\bar{v}\frac{\partial^{2}\bar{v}}{\partial\bar{r}^{2}}+\bar{u}\frac{\partial\bar{v}}{\partial r\,\partial x}\right)-4\left(\frac{\partial\bar{v}}{\partial\bar{r}}\right)^{2}-2\frac{\partial\bar{u}}{\partial\bar{r}}\left(\frac{\partial\bar{u}}{\partial\bar{r}}+\frac{\partial\bar{v}}{\partial\bar{x}}\right)\right. \quad (12)$$

$$\bar{\tau}_{xx}=4\eta_{0}\frac{\partial\bar{u}}{\partial x}-2k_{0}\left[2\frac{\partial^{2}\bar{u}}{\partial\bar{x}\,\partial t}+2\left(\bar{v}\frac{\partial^{2}\vec{u}}{\partial r\,\partial x}+u\frac{\partial^{2}\bar{u}}{\partial\bar{x}^{2}}\right)-4\left(\frac{\partial\bar{u}}{\partial\bar{x}}\right)^{2}-2\frac{\partial\bar{v}}{\partial\bar{x}}\left(\frac{\partial\bar{v}}{\partial x}+\frac{\partial\bar{u}}{\partial\bar{r}}\right)\right] \quad (13)$$

$$\tau_{rx}=\tau_{xr}=2\eta_{0}\left(\frac{\partial\bar{v}}{\partial\bar{x}}+\frac{\partial\bar{u}}{\partial\bar{r}}\right)-2k_{0}\left[\frac{\partial^{2}\bar{v}}{\partial x\,\partial t}+\frac{\partial^{2}\bar{u}}{\partial\bar{r}\,\partial\bar{t}}-2\frac{\partial\bar{v}}{\partial\bar{r}}\frac{\partial\bar{v}}{\partial\bar{x}}+\left(\bar{v}\frac{\partial}{\partial r}+\bar{u}\frac{\partial}{\partial x}\right)\right.$$
$$\left(\frac{\partial\bar{v}}{\partial\vec{x}}+\frac{\partial\bar{u}}{\partial\bar{r}}\right)-\frac{\partial\bar{u}}{\partial\bar{x}}\left(\frac{\partial\bar{v}}{\partial\bar{x}}+\frac{\partial\bar{u}}{\partial r}\right)-\frac{\partial\bar{v}}{\partial\bar{r}}\left(\frac{\partial\bar{v}}{\partial\bar{x}}+\frac{\partial\bar{u}}{\partial\bar{r}}\right)-2\frac{\partial\bar{u}}{\partial\bar{r}}\frac{\partial\bar{u}}{\partial x}\Big]. \quad (14)$$

3.1.Rate of volume flow and the boundary conditions

According to the relationship between the volumetric flow value and its average time rate, the corresponding boundary conditions will be dimensionless [7]:

$$F(x,t) = Q + 2(h(x,t) - 1). \tag{15}$$

$$\left.\begin{aligned} \psi &= \tfrac{F}{2} \text{ at } h_1 = 1 + \phi\cos\, 2\pi(x-t) \\ \psi &= -\tfrac{F}{2} \text{ at } h_2 = -1 - \phi\cos\, 2\pi(x-t) \\ \tfrac{\partial\psi}{\partial r} &= 1 \text{ at } r = h_1 \text{ and } r = h_2 \end{aligned}\right\}. \tag{16}$$

4.Perturbation analysis

Equation (11) shows that (P) depends on (x) only and it is nonlinear whivh means it is not easy to get a closed form solution, therefore to a void the value of (α), the marginal value problem is acceptable. For a simple analytical solution. In this way, the equations can be solved by proposing a small perturbation technique to solve non-linear problems after imposing the formulas below:

$$\left.\begin{aligned} \psi &= \psi_0 + \alpha\psi_1 \\ p &= p_0 + \alpha p_1 \\ \theta &= \theta_0 + \alpha\Theta_1 \end{aligned}\right]. \tag{17}$$

Substituting Equation (17) into Equations (10-11) then we have:

$$\frac{\partial P}{\partial r} = 0. \tag{18}$$

$$\frac{\partial P}{\partial x} = \frac{r+k}{k}\frac{\partial}{\partial r}\tau_{rx} + \frac{1}{r+k}H_a\frac{\partial\psi}{\partial r}. \tag{19}$$

$\tau_{xx} = 0, \tau_{rr} = 0.$

$$\tau_{rx} = 2\left(\frac{\partial^2\psi}{\partial x^2} - S^2\frac{\partial^2\psi}{\partial r^2} - 2k\left(S\frac{\partial^3\psi}{\partial x^2\,\partial t} - S^3\frac{\partial^3\psi}{\partial r^2\,\partial t} - 2S\frac{\partial^2\psi}{\partial r\,\partial x}\frac{\partial^2\psi}{\partial x^2}\right.\right.$$
$$\left.\left.+\delta\frac{\partial^3}{\partial x}\frac{\partial^3\psi}{\partial r\,\partial x^2} - \delta^3\frac{\partial\psi}{\partial x}\frac{\partial^3\psi}{\partial r^3} - \delta\frac{\partial\psi}{\partial r}\frac{\partial^3\psi}{\partial x^3} + \delta^3\frac{\partial\psi}{\partial r}\frac{\partial^3\psi}{\partial r^2\,\partial x} - 2\delta^3\frac{\partial^2\psi}{\partial r^2}\frac{\partial^2\psi}{\partial r\,\partial x}\right). \tag{20}$$

After performing the calculations, the power coefficient (α), will be obtained the two equations of zeroth and first order with it is boundary equations

4.1 Zeroth order equations: $\boldsymbol{\alpha^{(0)}}$

$$\frac{\partial P_0}{\partial x} = \frac{\partial}{\partial r}\left[\frac{(r+k)}{k}(\tau_{rx})_0\right] + \frac{1}{(r+k)}\,H_a\,\frac{\partial\psi_0}{\partial x},$$

where $(\tau_{rx})_0 = 2\frac{\partial^2\psi_0}{\partial x^2}$ (21)

Differentiating Equation (21) with respect to (r) implies to:

$$0 = 2\left(\frac{r+k}{k}\right)\frac{\partial^4\psi_0}{\partial x^4} + \frac{1}{(r+k)}H_a\frac{\partial^2\psi_0}{\partial x^2}, \tag{22}$$

with the corresponding boundary conditions:

$$\left.\begin{aligned} \psi_0 &= \tfrac{F_0}{2}, \tfrac{\partial\psi_0}{\partial x} = 1 \qquad \text{at } x = h_1 \\ \psi_0 &= -\tfrac{F_0}{2}, \tfrac{\partial\psi_0}{\partial x} = 1 \qquad \text{at } x = h_2 \end{aligned}\right]. \tag{23}$$

4.2 First order equations: $\boldsymbol{\alpha^{(1)}}$

$$\frac{\partial P_1}{\partial x} = \left(\frac{r+k}{k}\right)\frac{\partial}{\partial r}(\tau_{rx})_1 + \frac{1}{(r+k)}H_a\frac{\partial\psi_1}{\partial x}. \tag{24}$$

Where

$$(\tau_{rx})_1 = 2\frac{\partial^2\psi_1}{\partial x^2} - 2k\left[\frac{\partial\psi_0}{\partial x}\frac{\partial^3\psi_0}{\partial r\,\partial x^2} - \frac{\partial\psi_0}{\partial r}\frac{\partial^3\psi_0}{\partial x^3} - 2\frac{\partial^2\psi_0}{\partial r\,\partial x}\frac{\partial^2\psi_0}{\partial x^2}\right] \tag{25}$$

Differentiating Equation (24) with respect to (r), we get:

$$0 = \frac{\partial^4\psi_1}{\partial x^4} - k\frac{\partial^2}{\partial x^2}\left[\frac{\partial\psi_0}{\partial x}\frac{\partial^3\psi_0}{\partial r\,\partial x^2} - \frac{\partial\psi_0}{\partial r}\frac{\partial^3\psi_0}{\partial x^3} - 2\frac{\partial^2\psi_0}{\partial r\,\partial x}\frac{\partial^2\psi_0}{\partial x^2}\right] + \frac{k}{2(r+k)^2}H_a\frac{\partial^2\psi_1}{\partial x^2}. \tag{26}$$

The corresponding boundary conditions are:

$$\left.\begin{array}{ll} \psi_1 = \frac{F_1}{2},\ \frac{\partial \psi_1}{\partial x} = 1 & \text{at } x = h_1 \\ \psi_1 = -\frac{F_1}{2},\ \frac{\partial \psi_1}{\partial x} = 1 & \text{at } x = h_2 \end{array}\right]. \tag{27}$$

Using the mathematics program "MATHEMATICA", the solution was found in the following image:

$$\boldsymbol{\psi_0} = C[3] + xC[4] - \frac{\sqrt{2}(k+r)\left(\frac{\sqrt{2}(k+r)C[1]\mathrm{Cos}\left[\frac{\sqrt{\mathrm{Ha}}\sqrt{k}x}{\sqrt{2}(k+r)}\right]}{\sqrt{\mathrm{Ha}}\sqrt{k}} + \frac{\sqrt{2}(k+r)C[2]\mathrm{Sin}\left[\frac{\sqrt{\mathrm{Ha}}\sqrt{k}x}{\sqrt{2}(k+r)}\right]}{\sqrt{\mathrm{Ha}}\sqrt{k}}\right)}{\sqrt{\mathrm{Ha}}\sqrt{k}}$$

$$\begin{aligned} \boldsymbol{\psi_1} = A[3] + xA[4] &- \frac{1}{36\mathrm{Ha}^{3/2}k(k+r)}\Bigg(9\sqrt{\mathrm{Ha}}\Big(\mathrm{C1C4}k(3k^2+6kr+3r^2+\mathrm{Ha}kx^2) \\ &+ (k+r)\big(\sqrt{2}\mathrm{C2C4}\sqrt{\mathrm{Ha}}k^{3/2}x + 8(k+r)^2A[1]\big)\Big)\mathrm{Cos}\left[\frac{\sqrt{\mathrm{Ha}}\sqrt{k}x}{\sqrt{2}(k+r)}\right] \\ &+ 8\sqrt{k}(k+r)^2\big(20\sqrt{2}\mathrm{C1C2}(k+r) + 3\mathrm{C1}^2\sqrt{\mathrm{Ha}}\sqrt{k}x \\ &- 3\mathrm{C2}^2\sqrt{\mathrm{Ha}}\sqrt{k}x\big)\mathrm{Cos}\left[\frac{\sqrt{2}\sqrt{\mathrm{Ha}}\sqrt{k}x}{k+r}\right] \\ &+ \Bigg(9\sqrt{\mathrm{Ha}}\Big(\mathrm{C2C4}k(3k^2+6kr+3r^2+\mathrm{Ha}kx^2) \\ &+ (k+r)\big(-\sqrt{2}\mathrm{C1C4}\sqrt{\mathrm{Ha}}k^{3/2}x + 8(k+r)^2A[2]\big)\Big) \\ &- 32\sqrt{k}(k+r)^2\big(5\sqrt{2}\mathrm{C1}^2(k+r) - 5\sqrt{2}\mathrm{C2}^2(k+r) \\ &- 3\mathrm{C1C2}\sqrt{\mathrm{Ha}}\sqrt{k}x\big)\mathrm{Cos}\left[\frac{\sqrt{\mathrm{Ha}}\sqrt{k}x}{\sqrt{2}(k+r)}\right]\Bigg)\mathrm{Sin}\left[\frac{\sqrt{\mathrm{Ha}}\sqrt{k}x}{\sqrt{2}(k+r)}\right]\Bigg). \end{aligned}$$

5. Result and discussion

We will discuss some of the important features that have been described, namely the characteristic of the Peristaltic flow function and velocity axial distribution characteristic, it is worth noting that we will focus on the effects of the small Brinkman number and the curvature parameter (k). First, we will discuss the wonderful picture of how the flow properties change with the rheology of the Walter's-B fluid and the curvature of the channel, as this function works to trap an amount of non -Newtonian fluid inside the channel with flexible walls, where the bodies moves in the direction of the wave propagation. Figures $(2, 9)$ were drawn for the Parameters $(k, \phi, Ha, x, a, b, d^*)$ and, F_0 respectively, Figures$(3, 5)$, show that the blocked and trapped bolus gradually decreases with increasing parameters (ϕ) and (α) near the walls of the channel and further away fromit, while Figures (2, 4, 6, 7 and 9), show that there is an increasing in the number of boluses and their size with increasing parameters (k, Ha, a, b, and F_0), respectively, which thus shows a behaviour of parameter (d^*) lead to slight change value or each bolus and this is appear in Figure (8).

The velocity function (U) indicates the variation in the distribution of an axial velocity along the walls of the curved peristaltic channel. The effect of parameter values $k, H_a d, \alpha, a, d^*, b$ and F_0, on the axial velocity is shown in Figures $(10, 17)$. We have Figures 11 and 15 displayed that the axial velocity exhibits oscillation behavior with an increase in the parameters Ha and d^*, the velocity axial increasing toward the upper wall of curved

channel. The velocity profile decreases during the channel, and the effect of parameters ϕ, b and f_0 are sketched in Figures (12, 16 and 17), reduction behavior for velocity distribution is recognized as ϕ, b and f_0 increases. The impact of curvature parameter k on the axial velocity is explained in Figure (10), the velocity function decreases with all an enhancement of parameter k values near the upper wall of the channel and the opposite situation is reversed for the lower wall. In Figure (13) an increase in the power coefficient parameter (α), reduces the axil velocity profile toward the upper wall of the curved channel. From Figure (14) detected that the radius of stationary curved channel (a) attains maximum value in the core part of the curved channel then it becomes retarding toward the channel walls at the graphical model parameter (K), we find that at $0.3 < \mu < 0.7$ the velocity axial distribution inhenct. With the increase in the curvature of the channel (k) and decreases with the increase in curvature for all other values, noting that the function (U) is asymmetric for all small values of the curvature parameter (k) in the curved peristaltic channel.

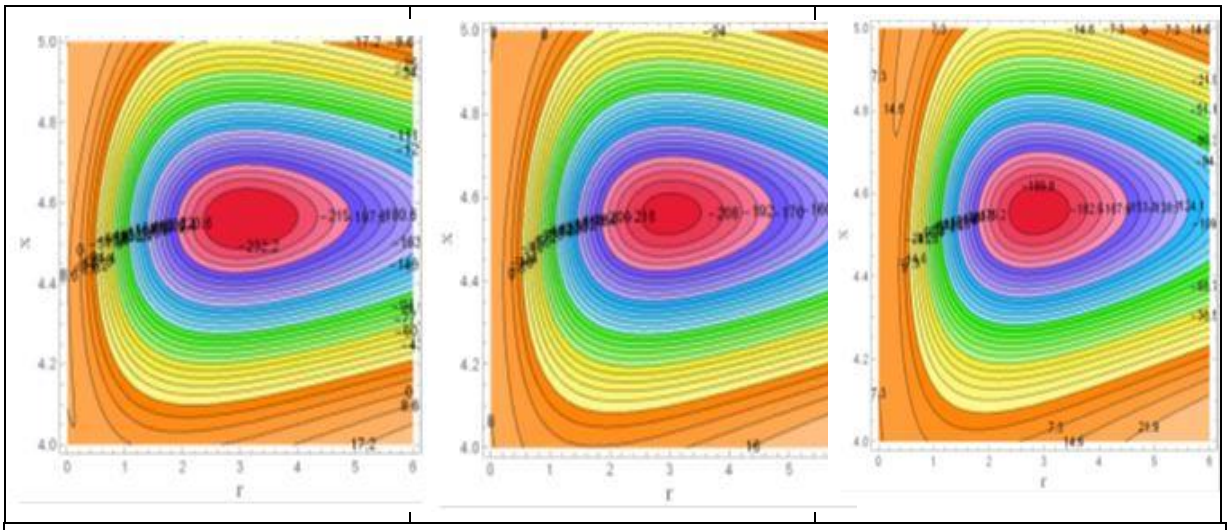

Figure2. Behavior of (k) in the wave frame for the sketch of stream function with ($k \to 1.5, \phi \to 0.4, Ha \to 0.9, \alpha \to 0.1, a \to 7, b \to 7, d^* \to 17, F0 \to 0.3$)

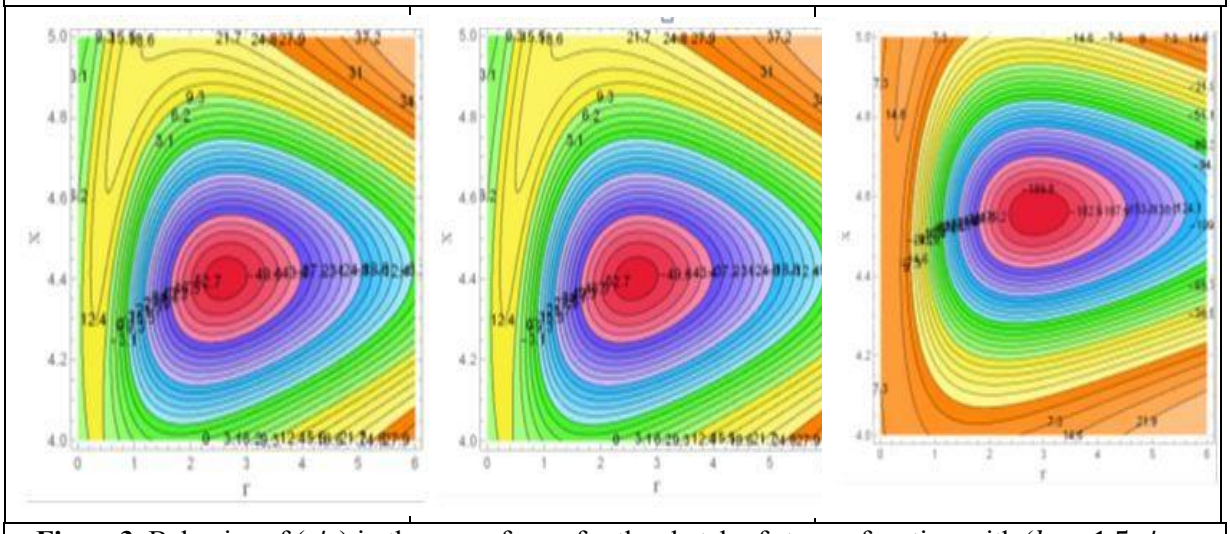

Figure3. Behavior of (ϕ) in the wave frame for the sketch of stream function with ($k \to 1.5, \phi \to 0.4, Ha \to 0.9, \alpha \to 0.1, a \to 7, b \to 7, d^* \to 17, F0 \to 0.3$)

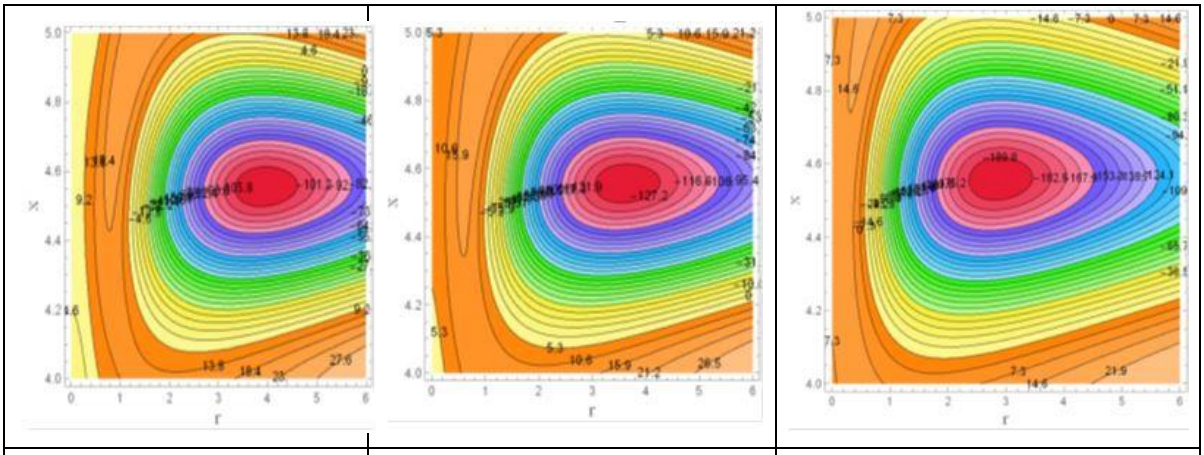

Figure 4: Behavior of (Ha) in the wave frame for the sketch of stream function with $(k \to 1.5, \phi \to 0.4, Ha \to 0.9, \alpha \to 0.1, a \to 7, b \to 7, d^* \to 17, F0 \to 0.3)$

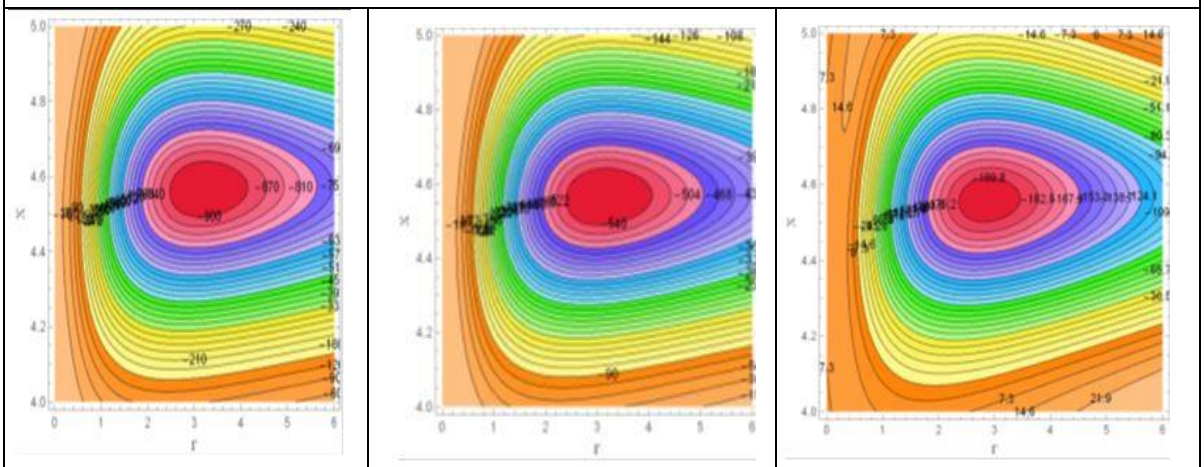

Figure 5: Behavior of (α) in the wave frame for the sketch of stream function with $(k \to 1.5, \phi \to 0.4, \mathrm{Ha} \to 0.9, \alpha \to 0.1, a \to 7, b \to 7, d^* \to 17, \mathrm{F0} \to 0.3)$

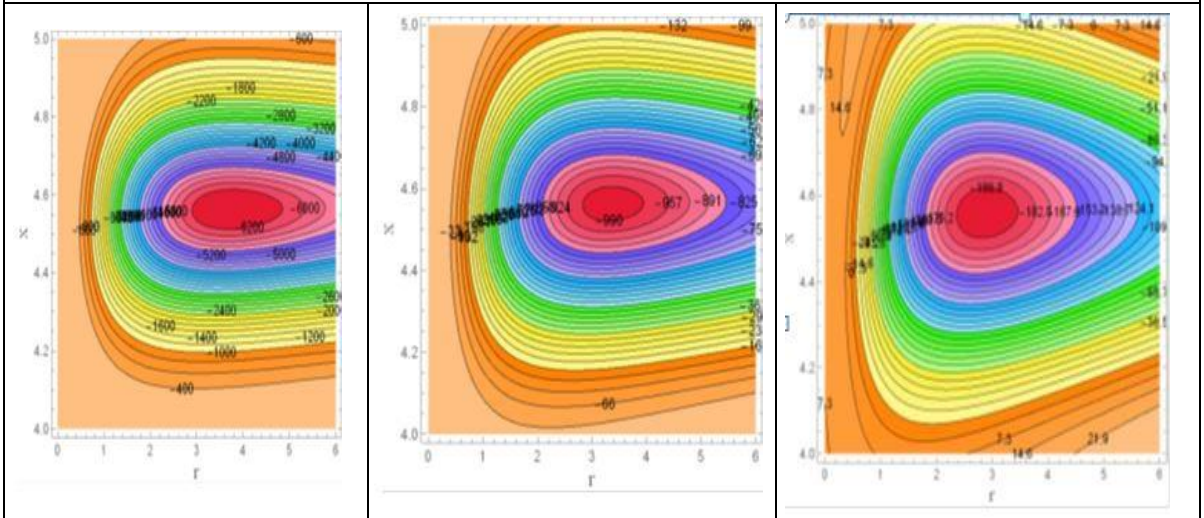

Figure 6: Behavior of (a) in the wave frame for the sketch of stream function with $(k \to 1.5, \phi \to 0.4, Ha \to 0.9, \alpha \to 0.1, a \to 7, b \to 7, d^* \to 17, F0 \to 0.3)$

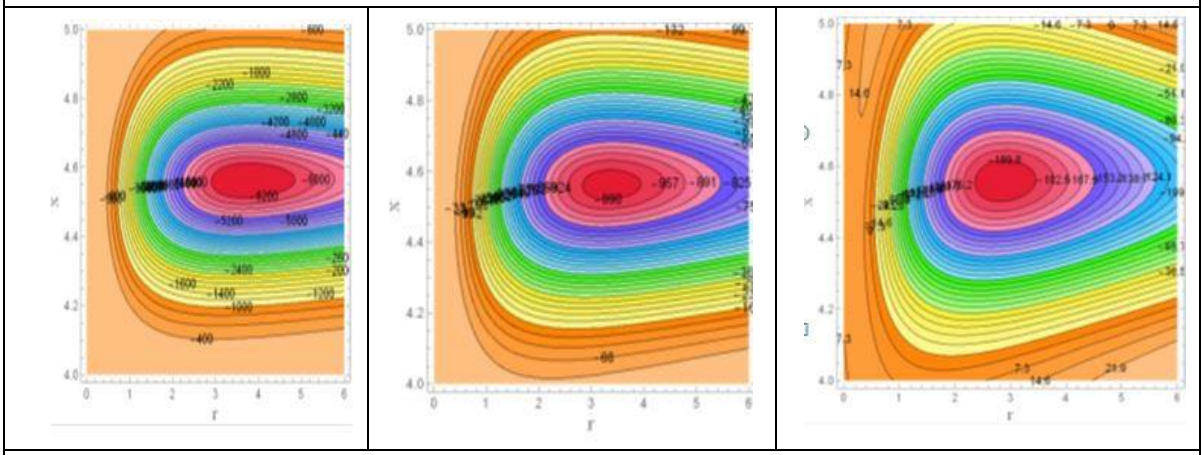

Figure 7: Behavior of (b) in the wave frame for the sketch of stream function with ($k \to 1.5, \phi \to 0.4, Ha \to 0.9, \alpha \to 0.1, a \to 7, b \to 7, d^* \to 17, F0 \to 0.3$)

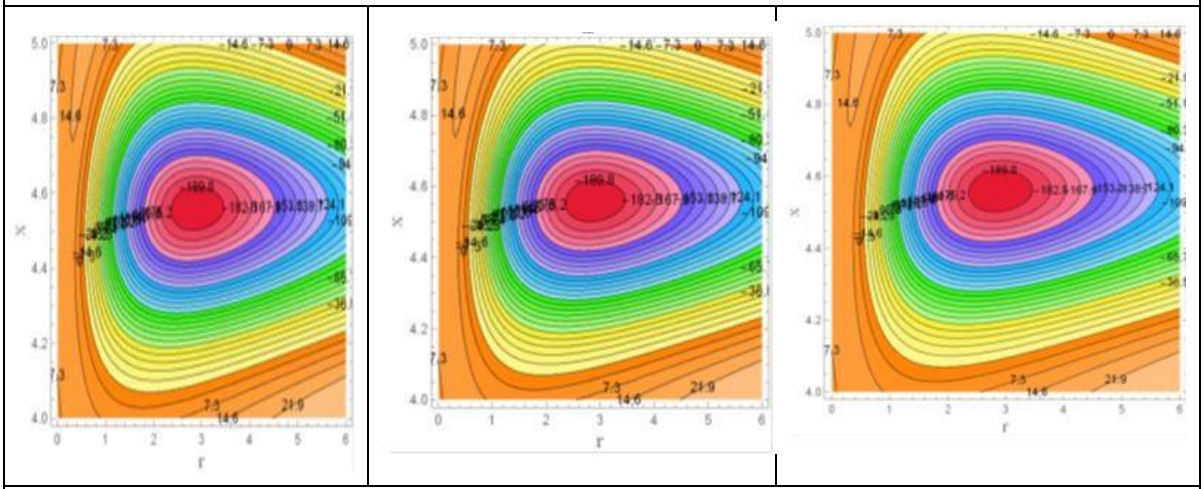

Figure 8: Behavior of (d^*) in the wave frame for the sketch of stream function with ($k \to 1.5, \phi \to 0.4, Ha \to 0.9, \alpha \to 0.1, a \to 7, b \to 7, d^* \to 17, F0 \to 0.3$)

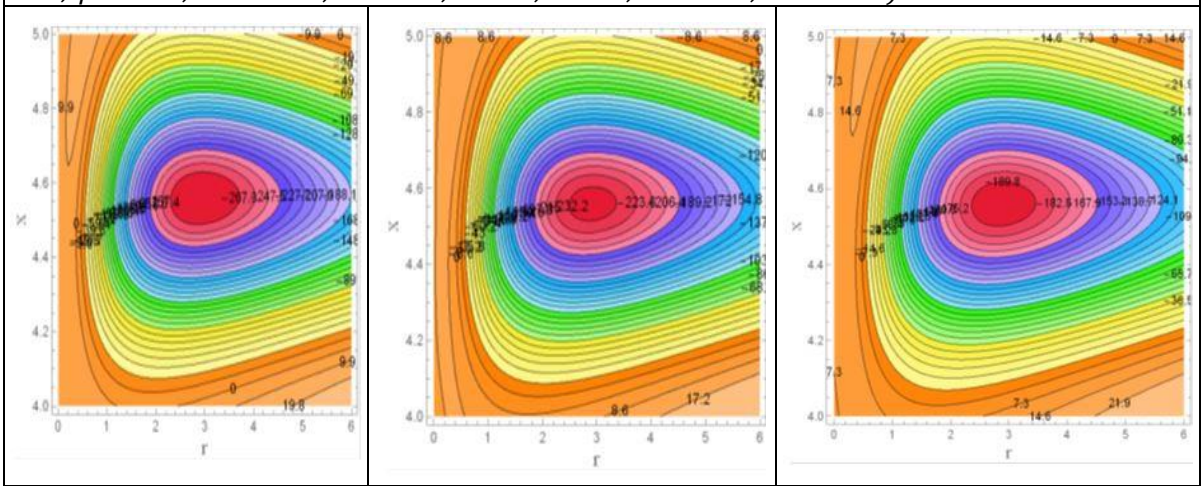

Figure 9: Behavior of (F_0) in the wave frame for the sketch of stream function with ($k \to 1.5, \phi \to 0.4, Ha \to 0.9, \alpha \to 0.1, a \to 7, b \to 7, d^* \to 17, F0 \to 0.3$)

5.2 Velocity distrubution

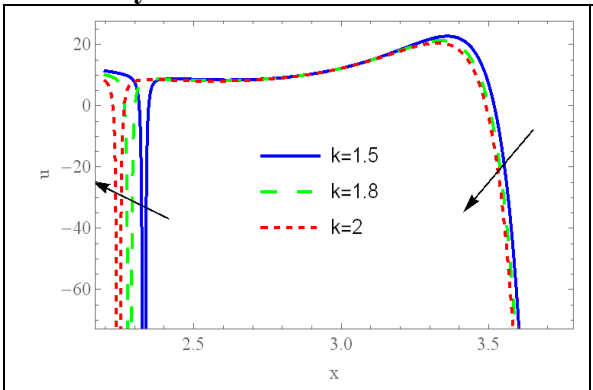

Figure 10: Behavior of (k) in the wave frame for the sketch of axial velocity distribution with $(\phi \to 0.2, \mathrm{Ha} \to 0.4, \alpha \to 0.1, a \to 9, b \to 9, d^* \to 16, \mathrm{F0} \to 0.3, r \to 1)$

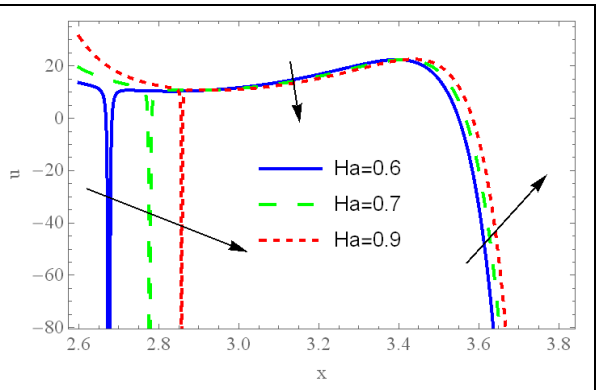

Figure11: Behavior of (Ha) in the wave frame for the sketch of axial velocity distribution with $(k \to 1.5, \phi \to 0.2, \alpha \to 0.1, a \to 9, b \to 9, d^* \to 16, \mathrm{F0} \to 0.3, r \to 1)$

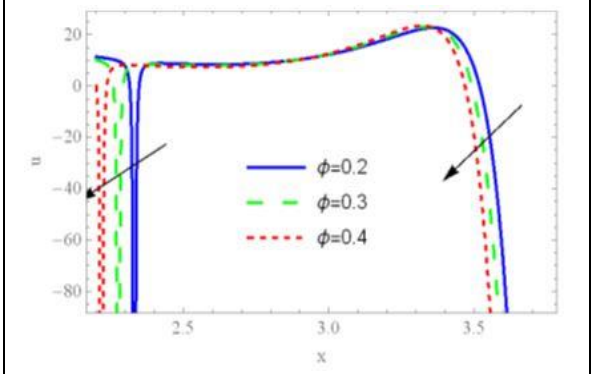

Figure 12: Behavior of (ϕ) in the wave frame for the sketch of axial velocity distribution with $(k \to 1.5, \mathrm{Ha} \to 0.4, \alpha \to 0.1, a \to 9, b \to 9, d^* \to 16, \mathrm{F0} \to 0.3, r \to 1)$

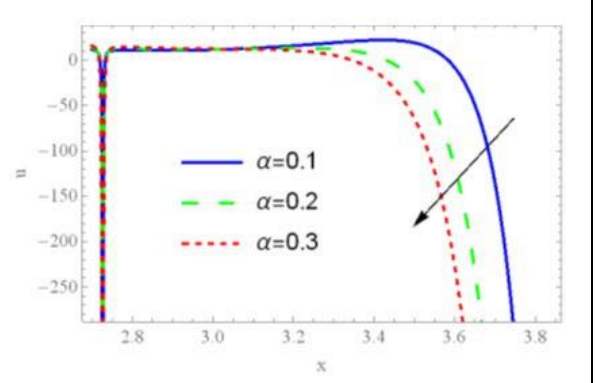

Figure 13: Behavior of (k) in the wave frame for the sketch of axial velocity distribution with $(k \to 1.5, \phi \to 0.2, \mathrm{Ha} \to 0.4, a \to 9, b \to 9, d^* \to 16, \mathrm{F0} \to 0.3, r \to 1)$

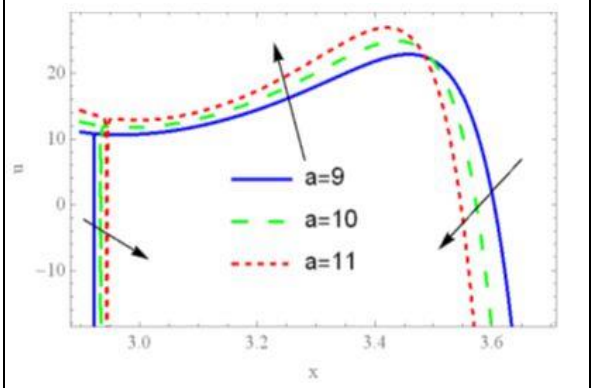

Figure14: Behavior of (a) in the wave frame for the sketch of axial velocity distribution with $(k \to 1.5, \phi \to 0.2, \mathrm{Ha} \to 0.4, \alpha \to 0.1, b \to 9, d^* \to 16, \mathrm{F0} \to 0.3, r \to 1)$

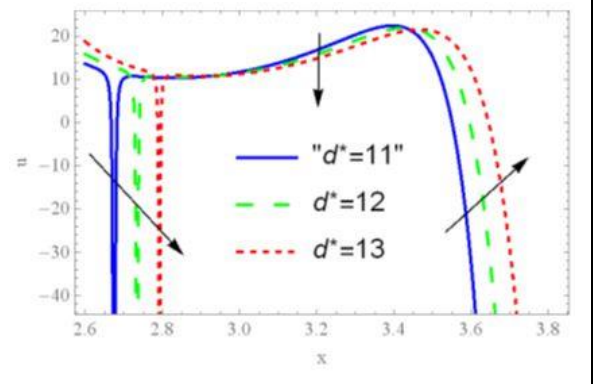

Figure15: Behavior of (d^*) in the wave frame for the sketch of axial velocity distribution with $(k1.5, \phi \to 0.2, \mathrm{Ha} \to 0.4, \alpha \to 0.1, a \to 9, b \to 9, \mathrm{F0} \to 0.3, r \to 1)$

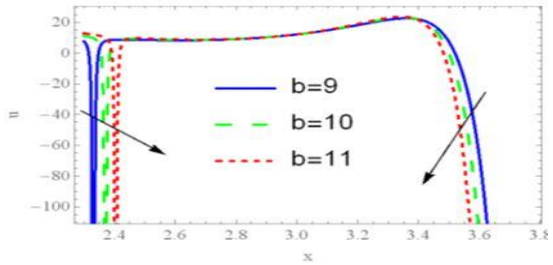

Figure16: Behavior of (b) in the wave frame for the sketch of axial velocity distribution with $(k \to 1.5, \phi \to 0.2, \mathrm{Ha} \to 0.4, \alpha \to 0.1, a \to 9, d^* \to 16, \mathrm{F0} \to 0.3, r \to 1)$

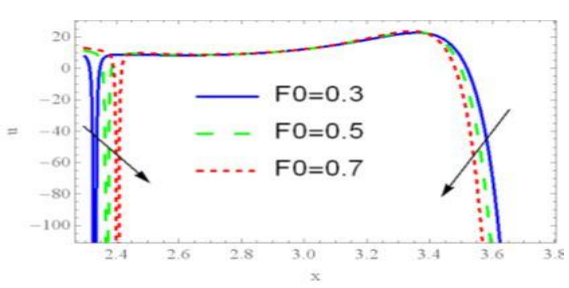

Figure17: Behavior of (F_0) in the wave frame for the sketch of axial velocity distribution with $(k \to 1.5, \phi \to 0.2, \mathrm{Ha} \to 0.4, \alpha \to 0.1, a \to 9, b \to 9, d^* \to 16, r \to 1)$

6.Conclusions

Mathematical modeling to study the effects of the magnetic field on the axial velocity and flow function of non-Newtonian Walter's- B fluid through curved peristaltic channels has been considered with a curved boundary walls. Impacts of different parameters on flow function and axial velocity distribution have been discussed graphically. Important features in the current analysis have been and discussed. In light of the results obtained in this study, we were able to indicate that the peristaltic flow in the curved channel of viscoelastic fluids, it is behavior clearly affects the movement and dynamics of the flow here, even though the flow is creeping.

The results showed that the flow rate of the non-Newtonian viscous fluid, represented by the Brinkman number, leads to the decrease in the pressure gradient- it was also shown that the curvature parameter (k) of the Walter's-B fluid is close to the effect of the Brinkman number. Moreover, the magnetic field applied from the outside is a good way to control the flow function provided that the flow rate is as small as possible. Let's take a look at the results the research reached in the following points:

- The effects of various parameters ($k, H_a, \phi, \alpha \ \ a_2 d^*, b, f_0$) appear to fluctuate on the flowfunction and the axial velocity distribution in the curved channel.
- The axial vela city values enhance and increase when the parameters values (d^* and Ha_a) increase.
- The profiles of the axial velocity and flow function appear to be parabolic and asymmetric for small values of the curvature parameter (k) of the curved peristaltic channel.
- The size and number of boluses clearly increase with increasing parameters (k, H_a, a, b, f_0) and decrease with increasing parameters (ϕ, α, d^*).
- The impact of inclusion parameter (amplitudes ratio $), a clear specificity over the axial velocity, where fluctuations are observed in the graph of this parameter.
- We can point out that the stream lines close to the channel walls are clearly traced when graphing shapes to the wall waves, which are generated mainly by the relative movement of the channel walls. We have noticed that the size and number of the boluses increases proportionally when the quality of the values of the most commonly used information increases here.

Refrences

[1] G. M. Moatimid and M. H. Zekry, "Nonlinear stability of electro-visco-elastic Walters' B type in

porous media," *Microsystem Technologies.,* vol. 26, pp. 2013 2027, 2020.

[2] R. G. Ibraheem and L. Z. Hummady, "Effect of Couple-stress with Slip Condtion and Rotation on Peristaltic Flow of a Powell-Eyring Fluid with the Influence of an Inclined Asymmetric Channel with Porous Medium," *Journal of Basic Sciences.,* vol. 10, no. 17,pp. 363-389, 2023.

[3] Z. A. Jaafar, L. Z. Hummady and M. H. Thawi, "Influence of Some Fluid Mechanic Parameters Caused From Heat Transport With Rotation on Walters, B Fluid," *Journal of Biomechanical Science and Engineering.,* vol. 18, no. 2, pp., 1-13, 2023.

[4] P. Sarkar and K. P. Madasu, "Parallel and perpendicular flows of a couple stress fluid past a solid cylinder in cell model: Slip condition," *Physics of Fluids,* vol. 35, no. 3, pp. 033101, 2023.

[5] A. Saleem, S. Akhtar, F. M. Alharbi, S. Nadeem, M. Ghalambaz, and A. Issakhov, "Physical aspects of peristaltic flow of hybrid nano fluid inside a curved tube having ciliated wall," *Results in Physics.,* vol. 19, pp. 103431, 2020.

[6] H. Sato, T. Kawai, T. Fujita, and M. Okabe, "Two dimensional peristaltic flow in curved channels," *Transactions of the Japan Society. Mech. English.,* vol. 66, no.4 pp. 679–688, 2000.

[7] F. ÖZBAĞ, "Numerical simulations of traveling waves in a counterflow filtration combustion model," *Turkish Journal of Mathematics.,* vol. 46, no. 4, pp. 1424 1435, 2022.

[8] V. K. Narla, K. M. Prasad, and J. V Ramanamurthy, "Peristaltic transport of Jeffrey nanofluid in curved channels," *Procedia Engineering.,* vol, 127, pp.869-876, 2015.

[9] Hana Lafta, S. Khalil, A.M., Abdulhadi, and M.H. Thawi, "The Impact of Rotation and Induced Magnetic Fields on Electroosmosis-Augmented Magnetohydrodynamic Peristaltic Transport," *International Conference on Mathematical and Statistical physics, Computational science, Education and communication .,* vol. 13941, pp. 1394112–15, 2025.

[10] Hana I. Lafta ,Zainab A. Jaafar and Rana G. Ibraheem, "Effect of a rotating Frame on Peristalsis Flow of a Walter's B Fluid Model Suspension in a Porous Medium, Physical Survey," *Journal of Natural and Applied Sciences URAL., vol.1, no.5, pp. 5-17, 2024.*

[11] Taha H. Jasim, Hana I. Lafta and Shaymaa M. Abdullah, "Some Types of Separation Axioms for (k, m) Generalized Fuzzy -(resp., fuzzy)- Closed Sets in Dfts," *Journal of Interdisciplinary Mathematics.,* vol.24, no.7, pp. 1787-1798 , 2021.

[12] Z. A. Jaafar, M. H. Thawi and L. Z. Hummady, "Impact of Couple Stress with Rotation on Walters, B Fluid in Porous Medium," *Iraqi Journal For Computer Science and Mathematics.,* vol. 4, no. 2, pp. 189–201, 2023.

[13] N. F. Okechi and S. Asghar, "Fluid motion in a corrugated curved channel," *The European Physical Journal Plus.,* vol. 134, no. 4, pp. 165, 2019.

[14] A. Kalantari, A. Riasi, and K. Sadeghy, "Peristaltic flow of giesekus fluids through curved channels: an approximate solution," *Nihon Reoroji Gakkaishi.,* vol. 42, no. 1, pp. 9–17, 2014.

[15] A. A. Khan, "Peristaltic movement of a dusty fluid in a curved configuration with mass transfer," *Punjab University Journal of Mathematics.,* vol. 53, no. 1, pp.55-71, 2021.

[16] A. A. Khan, S. Zafar, and A. Kanwal, "Effect of relaxation and retardation times on dusty Jeffrey fluid in a curved channel with peristalsis," *Advances in Mechanical Engineering.,* vol. 13, no. 6, p. 1-10, 2021.

[17] M. Faizan, S. S. Zafar, F. Ali, S. A. Lone, and A. Saeed, "Modeling of magneto bioconvection Williamson nanoliquid through modified heat flux: the significance of entropy," *Partial Differential Equations in Applied Mathematics.,* vol.10, pp. 100746, 2024.

[18] S. A. Lone, L. A. AL-Essa, H. Alrabaiah, F. Ali, H. Yasmin, and A. Saeed, "A numerical investigation of the chemically reactive maxwell nanofluid flow over a convectively heated rotating disk using Darcy–Forchheimer porous medium," *Modern Physics Letters B.,* vol.10, pp. 2450450, 2024.

[19] C. Srinivas Reddy, F. Ali, and M. F. A. F. Ahmed, "Aspects on unsteady for MHD flow of Cross nanofluid having gyrotactic motile microorganism due to convectively heated sheet," *Taylor & Francis. nternational Journal of Ambient Energy.,* vol. 43, no. 1, pp. 6028–6040, 2022.